Supporting Information

Scherzer et al. 10.1073/pnas.1507810112

SI Text

1. Transcriptional Regulation of Dionaea's Potassium Uptake Modules. ***Expression pattern of DmKT1 and DmHAK5.*** In our expression studies, we find DmKT1 as well as DmHAK5 expressed in the petiole, trap, and glands, with the DmKT1 expression level higher in glands and traps compared with the DmHAK5 expression level under nonstimulated conditions (Fig. S3). Thus, the basal expression level of DmKT1 might be responsible for the K^+-dependent depolarization of unstimulated gland cells in the low-affinity range (Fig. 1*D*). On trap stimulation, either by an insect or with the touch hormone mimic COR, transcript numbers of the transporter DmHAK5 increased 6-fold in traps and 18-fold in glands. In contrast, the K^+-channel DmKT1 was only slightly induced by stimulation (Fig. S3*B*).

DmHAK5 expression and high-affinity K^+ uptake show a similar time-dependent behavior. To study the time dependency in *Dionaea*'s K^+ uptake system, we analyzed the expression level of DmHAK5 after COR stimulation. As we already observed (Fig. S3*B*), DmHAK5 expression under unstimulated conditions was very low (Fig. S1*B*). Interestingly, its expression reaches a maximum 3.5 h after stimulation by COR and stays at this level for 2 d. When we analyzed the time dependency of high-affinity K^+ uptake in the *Dionaea* gland system, we were technically not able to detect any response to 0.03 mM K^+ during the first 3.5 h after stimulation. First depolarization was detected after 6 h, reaching the maximal K^+ uptake after 24 h (Fig. S1*B*). The delay between transcriptional induction and plasma membrane response is probably explained by the posttranslational machinery, which is necessary to incorporate the active protein into the plasma membrane.

2. DmHAK5 Acts as a Transporter. Carrier-mediated transport processes can be distinguished from a Nernstian-type ion channel based on their activation energy Q_{10}. To determine the Q_{10} of DmHAK5, we calculated the temperature dependence between 10 °C and 30 °C of the K^+/H^+ current amplitude. This temperature change affected the DmHAK5-dependent currents strongly (Fig. S6), and the Q_{10} value of 6.87 ± 1.06 (activation enthalpy was 38 kJ/mol) derived from Arrhenius plotting classifies the gland cell high-affinity K^+ transport activity as carrier-like. This result supports the notion of a K^+/H^+ symport mechanism by DmHAK5.

3. Estimation of the Relative Open Probability. Voltage-gated ion channels can exist in three functional states: closed, open, and inactivated (1). Although the closed and inactivated states are nonconductive states, the open conformation is conductive, mediating ion currents. In the case of DmKT1, prolonged hyperpolarization of the cell membrane shifts the channel into its open state (Fig. S4*C*). The relative open probability (rel. P_O) is a measure that determines the fraction of channels in the open/conductive state (1, all channels are open; 0, all channels are closed). The voltage-dependent gradual shift of rel. P_O from zero to one obeys a Boltzmann distribution. To determine rel. P_O, oocytes were successively challenged with voltage pulses ranging from +60 to −140 mV. When the channel-mediated currents reached equilibrium (steady state), the membrane potential was instantaneously changed to a constant voltage of +10 mV. Because the change in membrane potential is faster than the decay of the channels' open probability, the instantaneous currents (I_{inst}) right after the voltage jump represent a measure for the open probability of the steady-state conditions at the preceding membrane potential. When plotting I_{inst} as a function of voltage, a Boltzmann equation (below) can be used to describe the data and determine channel characteristics, like the voltage where the half-maximal open probability is reached:

$$\frac{P}{P_O + P_c} = \frac{1}{1 + \exp\left(\frac{(V - V_{0.5}) \times z \times e_0}{k \times T}\right)}.$$

P_O and P_c are the fractional occupancies of the open and closed states, respectively. V is the membrane potential, and $V_{0.5}$ is the voltage at which one-half of the channels are in the open state; k is Boltzmann's constant, and z is the number of the moved electric charges $e_0 = 1.6 \times 10^{-19}$ C necessary for the channel to open. The temperature is $T = 290.6$ K.

SI Methods

Cloning of DmKT1 and DmHAK5. Inspection of the available EST data from *Dionaea muscipula* (2) revealed coding sequences related to potassium transporter homologs. PolyA-mRNA was isolated from 10 μg total RNA using Dynabeads (Invitrogen) according to the manufacturer's instructions. cDNA was generated from *D. muscipula* whole-plant mRNA. The cDNA of potassium transporters was amplified using gene-specific oligonucleotide primers, which comprised the coding DNA sequence (CDS) of DmKT1 (GenBank accession No. LN715171) and DmHAK5 (GenBank accession no. LN715172) and Advantage cDNA Polymerase Mix (Clontech), revealing a sequence identical to that expected from the EST data. The full-length clones were inserted into pGEM-T Easy using the pGEM-T Easy Vector System I (Promega). For heterologous expression in *Xenopus* oocytes, the generated cDNAs were cloned into oocyte expression vectors (based on pGEM vectors) by an advanced uracil excision-based cloning technique described by Nour-Eldin et al. (3). For functional analysis, cRNAs were prepared using the mMessage mMachine T7 Transcription Kit (Ambion). Oocyte preparation and cRNA injection have been described elsewhere (4). For oocyte electrophysiological experiments, 25 ng potassium transporter cRNA was injected.

Noninvasive Ion Flux Measurements. Microelectrodes with external tip diameters of ∼2 μm were pulled, silanized, and filled with an appropriate ion-selective mixture [K^+ 60031; Sigma; mixture was prepared as described in the work by Jayakannan et al. (5)]. Electrodes were then calibrated in an appropriate set of standards and mounted on a 3D micromanipulator (MMT-5; Narishige). An immobilized lobe was placed into a 90-mm Petri dish containing 40 mL basic salt media (BSM; 0.2 mM KCl, 0.1 mM $CaCl_2$ adjusted to required pH using MES/Tris) and then, placed into a Faraday cage. The K^+-selective microelectrode was positioned with the tip aligned 50 μm above the lobe surface using a 3D hydraulic manipulator. During the measurements, a computer-controlled stepper motor moved electrodes in a slow (10 s) square-wave cycle between the two positions: close to (50 μm) and away from (150 μm) the trap surface. The potential difference between two positions was recorded by the MIFE CHART software (6) and converted into electrochemical potential difference using the calibrated Nernst slopes of the electrodes. Net ion fluxes were calculated using the MIFEFLUX software for cylindrical diffusion geometry (7).

To study the dose dependence of K^+ uptake, intact *Dionaea* leaves were pretreated with COR for 24 h as described above. A single lobe was cut and immobilized in a measuring chamber by

using medical adhesive (VH355; Ulrich AG). The lobe was left for adaptation in BSM solution before flux measurements started. Net K^+ fluxes were measured in response to consecutive increases in KCl content in the external BSM (KCl: 10, 50, 100, 200, 1,000, and 10,000 μM) during 3 min at each KCl concentration. The pH of the media was maintained at pH 4. Traps without COR treatment were used as controls. To address pH dependence of the studied channel, K^+ fluxes were recorded at pH 4 and 8 at two KCl levels (10 and 200 μM).

Intracellular Measurements. In the course of experiments, leaves were constantly perfused with the standard solution (1 mL/min). For stimulation, a 1-min exposure to the respective KCl concentration was sufficient. For impalements, microelectrodes from borosilicate glass capillaries with filament (Hilgenberg) were pulled on a horizontal laser puller (P2000; Sutter Instruments Co.). They were filled with 300 mM KCl and connected through an Ag/AgCl half-cell to a head stage (1 GΩ; HS-2A; Axon Instruments). Tip resistances were about 30 MΩ. Reference electrodes were filled with 300 mM KCl as well. An IPA-2 Amplifier (Applicable Electronics, Inc.) was used. The cells were impaled using an electronic micromanipulator (NC-30; Kleindiek Nanotechnik).

Oocyte Recordings. In double-electrode voltage-clamp studies, oocytes were perfused with citric acid/Tris-based buffers. The standard bath solution contained 10 mM citric acid/Tris (pH 4), 1 mM $CaCl_2$, 1 mM $MgCl_2$, and 1 mM $LaCl_3$. Osmolality of each solution was adjusted to 220 mOsm/kg using D-sorbitol. To balance ionic strength for measurements under varying cation concentrations, we compensated with lithium for a total concentration of 100 mM. Solutions for selectivity measurements of DmKT1 were composed of standard bath solution supplemented with 100 mM Na^+, $NMDG^+$, NH_4^+ Li^+, K^+, Rb^+, or Cs^+ chloride salts. For selectivity measurements of the high-affinity DmHAK5 transporter, respective cations were used at a concentration of 2 mM, and osmolarity was adjusted to 220 mOsm/kg using D-sorbitol. For analyzing the pH dependency, the pH value of standard solutions was adjusted between pH 7 and 6 with the MES/Tris buffer system. For pH values between pH 5.5 and 3, 10 mM citric acid instead of MES was used. Temperature experiments were performed under standard solution conditions as described by Scherzer et al. (8). For current–voltage relations (IV curves), single-voltage pulses were applied in 10-mV decrements from +60 to −140 mV starting from a holding potential (V_H) of 0 mV. Steady-state currents (I_{SS}) were measured at the end of test pulses lasting 100 ms in the case of DmHAK5 and 3 s in the case of DmKT1, and the cord conductance (G_K) was calculated according to

$$G_K = \frac{I_{ss}}{(V - V_{rev})}.$$

Here, V_{rev} is the reversal potential, which was determined from tail currents after a preactivation of −100 mV. Because currents were small in 5 mM K^+, we extrapolated the measured V_{rev} from 10 to 100 mM to calculate the V_{rev} for 5 mM K^+.

The calculation of the channel cord conductance eliminates the influence of the chemical driving force of the potassium gradient and was shown to result in a voltage-dependent conductance according to Geiger et al. (9):

$$G_{K-} = \frac{\frac{G_{max}}{(V - V_{rev})}}{\left(1 + \exp\left(\frac{zF\left(V - V_{1/2}\right)}{RT}\right)\right)}.$$

$V_{1/2}$ is the half-maximal activation voltage, z is the apparent gating charge, and G_{K-max} is the maximal cord conductance.

Data were analyzed using Igor Pro and Origin Pro-9.0G.

1. Karmazinova M, Lacinova L (2010) Measurement of cellular excitability by whole cell patch clamp technique. *Physiol Res* 59(Suppl 1):S1–S7.
2. Schulze WX, et al. (2012) The protein composition of the digestive fluid from the venus flytrap sheds light on prey digestion mechanisms. *Mol Cell Proteomics* 11(11): 1306–1319.
3. Nour-Eldin HH, Hansen BG, Norholm MH, Jensen JK, Halkier BA (2006) Advancing uracil-excision based cloning towards an ideal technique for cloning PCR fragments. *Nucleic Acids Res* 34(18):e122.
4. Escalante-Pérez M, et al. (2012) Poplar extrafloral nectaries: Two types, two strategies of indirect defenses against herbivores. *Plant Physiol* 159(3):1176–1191.
5. Jayakannan M, Babourina O, Rengel Z (2011) Improved measurements of Na^+ fluxes in plants using calixarene-based microelectrodes. *J Plant Physiol* 168(10):1045–1051.
6. Shabala SN, Newman IA, Morris J (1997) Oscillations in H^+ and Ca^{2+} ion fluxes around the elongation region of corn roots and effects of external pH. *Plant Physiol* 113(1): 111–118.
7. Shabala L, Ross T, McMeekin T, Shabala S (2006) Non-invasive microelectrode ion flux measurements to study adaptive responses of microorganisms to the environment. *FEMS Microbiol Rev* 30(3):472–486.
8. Scherzer S, et al. (2013) The Dionaea muscipula ammonium channel DmAMT1 provides NH_4^+ uptake associated with Venus flytrap's prey digestion. *Curr Biol* 23(17): 1649–1657.
9. Geiger D, et al. (2009) Heteromeric AtKC1middle dotAKT1 channels in Arabidopsis roots facilitate growth under K+-limiting conditions. *J Biol Chem* 284(32):21288–21295.

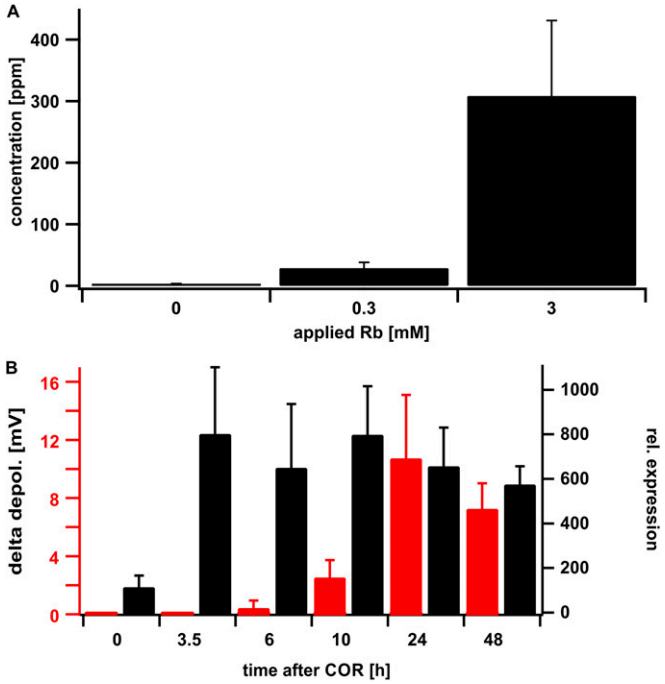

Fig. S1. Time-dependent activation of DmHAK5 in *Dionaea* traps. (*A*) Traps were fed with standardized insect powder, which was supplemented with RbCl at the given concentrations. Rb^+ uptake was analyzed 24 h after feeding onset. (*B*) The expression of DmHAK5 in *Dionaea* traps reaches a maximum 3.5 h after induction by COR (right axis). This expression rate stays at this level for 2 d. The high-affinity K^+-dependent depolarization in corresponding traps was measured by application of 30 μM K^+ (left axis). First depolarization was detected after 6 h, reaching the maximal K^+ uptake after 24 h (mean membrane depolarization ± SD; $n \geq 5$).

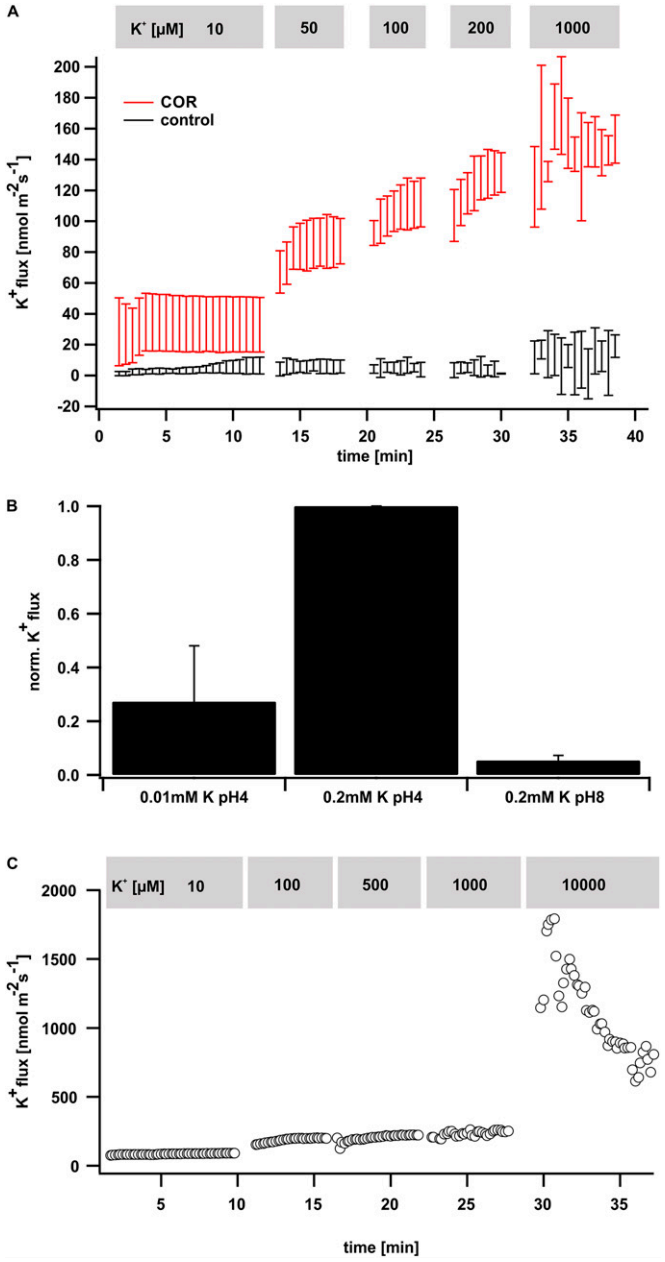

Fig. S2. Ion flux measurements across the membrane of *Dionaea* glands. (*A*) Time-dependent net K^+ fluxes measured with COR-stimulated (red) and non-stimulated (black) Venus flytrap glands in response to the indicated external K^+ concentrations. Stimulated traps showed K^+ influxes increasing with increasing external K^+ application. Nonstimulated traps showed no significant K^+ influx under identical conditions ($n \geq 7$; mean ± SD). (*B*) K^+ influx into *Dionaea* glands is H^+-dependent. Normalized K^+ fluxes from COR-stimulated Venus flytraps were measured in response to low (0.01 mM; left bar) and high (0.2 mM; center bar) KCl concentrations at pH 4. Increasing the external pH to 8 made the K^+ flux vanish at a K^+ concentration of 0.2 mM ($n \geq 8$; mean ± SD; right bar). (*C*) Representative experiment of a COR-stimulated Venus flytrap measured at K^+ concentrations in the high- and low-affinity ranges. With external K^+ up to 1 mM, a high-affinity uptake system was active, mediating K^+ influx of ~200 nmol m^{-2} s^{-1}. With 10 mM external K^+, high-capacity influx of up to 1,800 nmol m^{-2} s^{-1} was detected, indicating that, in addition to the high-affinity uptake, there is a low-affinity/high-capacity uptake system expressed in *Dionaea* glands.

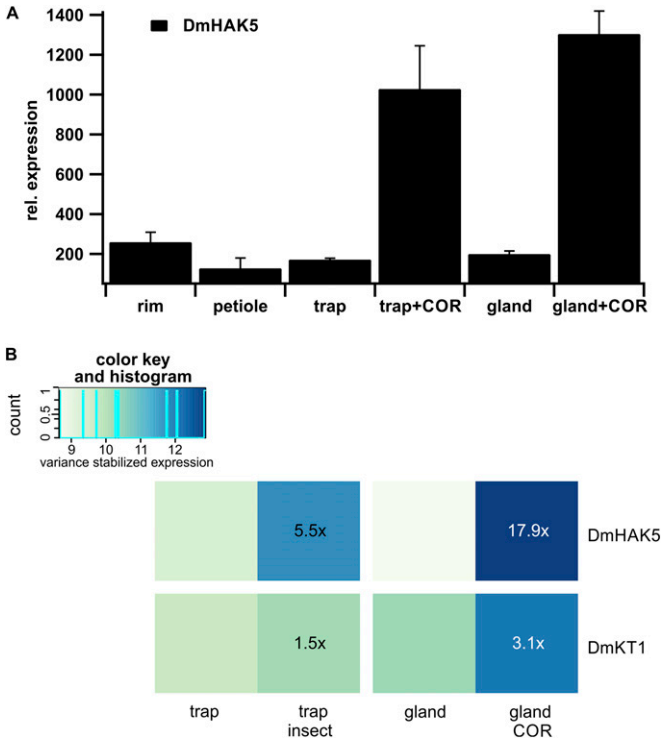

Fig. S3. Expression pattern of the K^+ uptake system in *Dionaea*. (*A*) Quantification of DmHAK5 transcript levels in different aerial tissues. DmHAK5 transcripts were normalized to 10,000 molecules of DmACT1 (*Dionaea* Actine1). Expression of the high-affinity K^+ transporter was strongly up-regulated by COR in traps and glands of *Dionaea* ($n = 3$; mean ± SE). (*B*) Quantification of DmHAK5 and DmKT1 transcript levels after stimulating traps of *Dionaea* with COR and feeding insects. Expression values are variance-stabilized for graphical exploratory analysis. Both DmHAK5 and DmKT1 are being induced during stimulation. Fold change and overall expression level are much higher for DmHAK5 after stimulation compared with DmKT1.

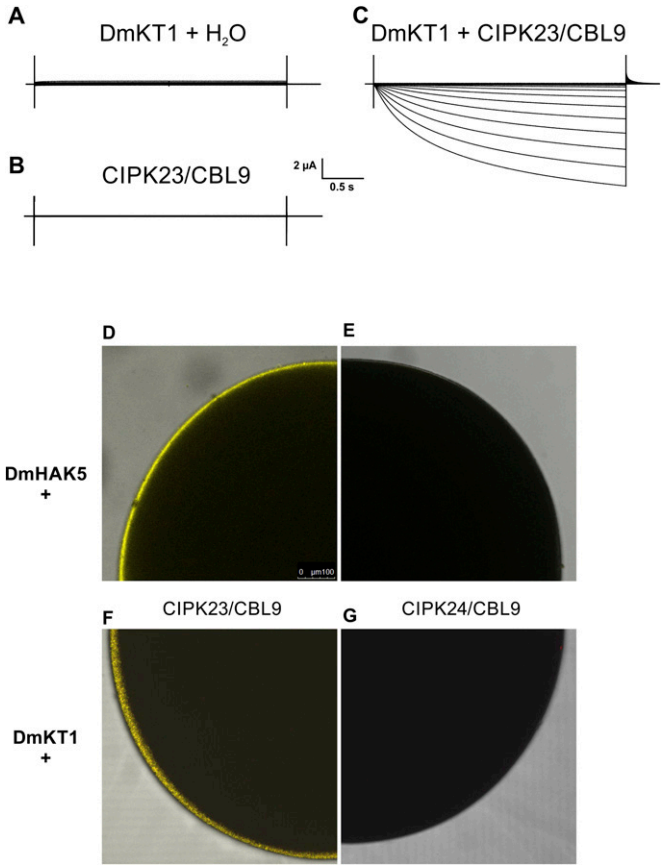

Fig. S4. CIPK23 interacts with and activates the *Dionaea* K^+ uptake system. Whole-oocyte voltage-clamp measurements of DmKT1 at membrane potentials ranging from +60 to −140 mV in 20-mV decrements in the presence of 100 mM KCl are shown. (*A*–*C*) Macroscopic K^+ currents of up to 12 µA were only detectable in oocytes coexpressing DmKT1 with CBL9 + CIPK23. (*D*–*G*) Bimolecular fluorescence complementation in *Xenopus* oocytes revealed physical interaction between (*D* and *E*) DmHAK5, (*F* and *G*) DmKT1, and (*D* and *F*) CIPK23/CBL9 but not (*E* and *F*) CIPK24/CBL9. Pictures taken with a confocal laser-scanning microscope show one-quarter of an optical slice of an oocyte. (*D*) DmHAK5::YFP^C coexpressed with CBL9 + CIPK23::YFP^N. (*E*) DmHAK5::YFP^C coexpressed with CBL9 + CIPK24::YFP^N. (*F*) DmKT1::YFP^C coexpressed with CBL9 + CIPK23::YFP^N. (*G*) DmKT1::YFP^C coexpressed with CBL9 + CIPK24::YFP^N.

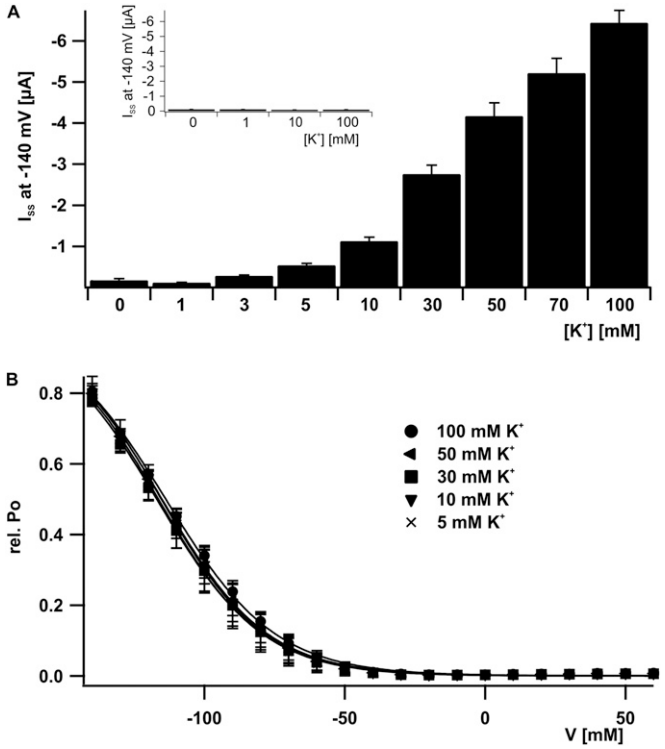

Fig. S5. Biophysical analysis of DmKT1-mediated K^+ currents at varying extracellular K^+ concentrations. (*A*) Steady-state currents of oocytes expressing DmKT1/CIPK23/CBL9 at pH 4 under different external K^+ concentrations recorded at −140 mV. The ionic strength of the solutions with varying K^+ concentrations was adjusted to 100 mM with Li^+. *Inset* shows currents of H_2O-injected control oocytes under the same conditions ($n = 5$; mean ± SD). (*B*) The relative open probability (rel. P_O) of DmKT1/CIPK23/CBL9 expressed in oocytes at an external pH of 4 was plotted against the test voltages. The data points were fitted with a Boltzmann function (solid lines; $n = 6$; mean ± SD). Note that K^+ is not affecting the half-maximal activation potential ($V_{1/2}$).

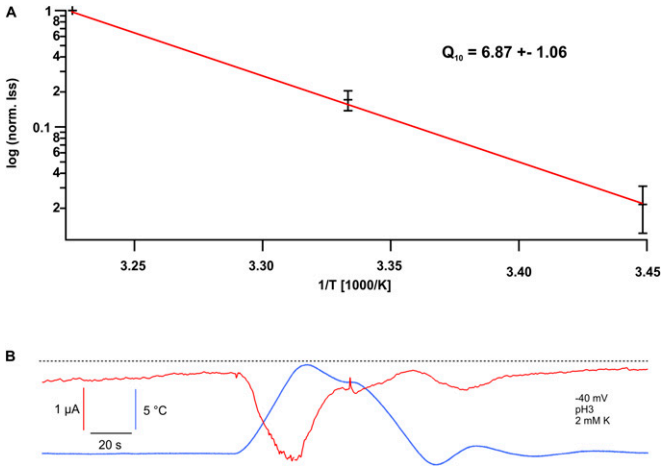

Fig. S6. Temperature dependency of DmHAK5. (*A*) DmHAK5/CIPK23/CBL9 functions as a transporter. Arrhenius plot of normalized currents recorded at 2 mM K^+ and a membrane potential of −140 mV at pH 3 and varying temperatures (as indicated). A mean Q_{10} value of 6.87 ± 1.06 was calculated at membrane potentials of −100 and −140 mV. Numbers represent a mean Q_{10} value of the currents recorded at 10–20 °C, 20–30 °C, and 10–30 °C ($n = 6$; mean ± SD). In a second approach, the linear regression in the Arrhenius plot with a slope of −4,588 ± 98 corresponds to an activation enthalpy E_a ($E_a = -R \times$ slope; R is the gas constant) of 38 ± 4 kJ/mol ($n = 6$; mean ± SD). (*B*) Temperature dependency of DmHAK5/CIPK23/CBL9-mediated K^+ currents. Representative measurements were performed at pH 3 and a membrane potential of −40 mV. Currents were induced by 2 mM K^+. Increasing the bath temperature from 20 °C to 30 °C (blue line) resulted in rapidly increasing inward currents (red line), which behavior was reversed by lowering the temperature to 20 °C again. The dotted line represents the zero current value.